sciendo

POLISH MARITIME RESEARCH 3 (115) 2022 Vol. 29; pp. 21-32
10.2478/pomr-2022-0024

FLOW FIELD CHARACTERISTIC ANALYSIS OF CUSHION SYSTEM OF PARTIAL AIR CUSHION SUPPORT CATAMARAN IN REGULAR WAVES

Jinglei Yang [1]
Han-bing Sun [2]*
Xiao-wen Li [1]
Xin Liu [1]

[1] Jimei University, School of Marine Engineering, Xiamen, China
[2] Harbin Engineering University, College of shipbuilding engineering, Harbin, China

* Corresponding author: *sunhanbing@hrbeu.edu.cn (H. Sun)*

ABSTRACT

In order to study the flow field characteristics of cushion system of partial air cushion support catamaran (PACSCAT) in waves, an analysis was carried out involving flexible treatment on the bow and stern air seals to simulate air seal shape under test conditions by means of computational fluid dynamics method and fluid structure interaction (FSI) method. On this basis, the pressure conditions of the air cushion chamber and the pressurized chamber at different wavelengths and different speeds are studied and compared with experimental results. The experimental results show that: for the air cushion pressure, the nonlinear characteristics of the numerical calculation results are more subtle than the experimental values, after linear transformation, the amplitudes of the experimental values are obviously greater than the calculated values after linear transformation, but the average values are not much different; At low speed of 2.0m/s, the spatial pressure distribution of the pressurized chamber and the air cushion chamber are uniformly distributed, at high speed of 3.6m/s, except for a certain pressure jump occurred in the air cushion chamber near the stern air seal, the pressure in other spaces is also evenly distributed, it proves that the pressurized chamber type of air intake can effectively meet the air cushion pressure balance.

Keywords: regular waves; partial air cushion support catamaran (PACSCAT); cushion system; fluid structure interaction (FSI); flow field characteristics

INTRODUCTION

The partial air cushion support catamaran (PACSCAT) is a new type of high-performance ship, which is based on slender catamaran and supported by air cushion [1-2]. It not only can sail at high speed with the attitude of planning boat, but also has outstanding sailing stability and maneuverability. Due to the wide sidewall of the PACSCAT, propellers or water jets can be used as propulsion devices, allowing PACSCAT to have better maneuverability than air cushion vehicle (ACV).

The non-uniform distribution of air cushion is a difficulty in studying the motion characteristics of hovercraft. So, it is necessary to establish a spatial non-uniform pressure distribution model of air cushion. In fact, the form of air cushion spatial distribution is closely related to the governing equation satisfied by aerodynamic force. The continuity equation is related to the spatial uniform distribution of the air cushion, the one-dimensional wave equation is related to the non-uniform distribution of the air cushion along the length direction, and the three-dimensional wave equation is related to the non-uniform pressure distribution of the air cushion in three dimensions. Obviously, it is the latter two governing equations that are more accurate to describe the spatial non-uniform pressure distribution characteristics of

air cushion. The hydrodynamic analysis software of the air cushion platform ACVSIM [3-4] and WAMIT [5], can be used to obtain the distribution characteristics of the air cushion in three-dimensional space. Of which, ACVSIM uses the three-dimensional wave equation directly as the governing equation of the air cushion flow field, and its numerical solution adopts the immersion boundary element method (IBM). The immersed boundary element method can allow the air cushion boundary to deform and is suitable for the air cushion with speed and arbitrary shape. On the other hand, WAMIT uses the method of transforming 3D wave equation into Helmholtz equation (assuming aerodynamic force as harmonic pulsation) as the governing equation of air cushion flow field, and its velocity potential is obtained by Fourier series solution which is applicable to rectangular air cushion (Lee and Neumann, (2016) [6]. Therefore, the establishment of the spatial non-uniform pressure distribution model can solve the heave, pitch and other motion problems of hovercraft, achieve accurate simulation of the aerodynamic force under any wave direction, and help to explain the unique resonance problems of hovercraft, such as "pebble" effect [7] or acoustic resonance phenomenon [8].

As a practical engineering method with wide application in the calculation of ship hydrodynamic, numerical method has been proved to be applicable to the simulation of hovercraft motion [9-11].In the simulating calculation of PACSCAT motion, the mechanical models are considered nonlinear except the fan characteristic equation which cannot completely simulate the fan pumping up, and the motion characteristics are also considered strongly nonlinear [12-13], which are highly consistent with the strong nonlinear phenomenon caused by multiple factors of PACSCAT. When the hovercraft is sailing in the waves, the pressure and flow field of the air-cushion system will change to a certain extent due to the nonlinear discharge, which will not only affect the movement performance, but also seriously affect the normal use of the hovercraft. Due to the high speed of the local air-cushion catamaran, the pressure and flow field characteristics of the air-cushion system have a crucial impact on the navigation performance. Therefore, the purpose of this paper is to study the pressure characteristics and air-cushion space of the cushion lift system in waves. distribution characteristics. The author conducts fluid structure interaction treatment on bow and stern flexible air seals of PACSCAT based on the fluid structure interaction solver of commercial hydrodynamic calculation software STAR-CCM+, and analyses the flow field characteristics of the cushion system based on fluid structure interaction method.

NUMERICAL CALCULATION METHOD

GOVERNING EQUATIONS AND THEORIES

For traditional computational fluid dynamics, numerical calculation for incompressible viscous flow and multiphase flow theory follows the Reynolds-Averaged Navier-Stokes equation [14-15], which is the most widely used in engineering. Ignoring the effect of density pulsation and considering the change of average density, the equation is as follows:

$$\frac{\partial \rho}{\partial t} + \frac{\partial}{\partial x_i}(\rho u_i) = 0 \tag{1}$$

$$\frac{\partial(\rho u_i)}{\partial t} + \frac{\partial}{\partial x_j}(\rho u_i u_j) = -\frac{\partial p}{\partial x_i} + \frac{\partial}{\partial x_j}\left[\mu \frac{\partial u_i}{\partial x_j} - \overline{\rho u_i' u_j'}\right] + S_i \quad (i, j = 1, 2) \tag{2}$$

Where, u_i, u_j is the time average value of the velocity component; i, j = 1, 2; ρ is fluid density; μ is hydrodynamic viscosity coefficient; u'_i, u'_j is the pulsation value of the velocity component; p is the time average value of pressure; S_i is the generalized source term of momentum equation.

This study uses VOF free liquid surface method [16-18] as the numerical simulation method of motion interface capturing, which is characterized by defining the motion interface as a fluid volume function in the spatial grid, and establishing the development equation of this fluid volume function, which makes the interface capturing problem is how to accurately determine the position, shape and deformation direction of the moving interface through fluid transport.

The motion model adopts the motion mode of six degrees of freedom (DFBI). The following is its motion equation. First, the motion equation of its center of gravity is established by the overall coordinate system, and its equation is:

$$m \frac{\mathrm{d}v}{\mathrm{d}t} = \vec{f} \tag{3}$$

where m is the mass of the hull, $\vec{f}$ is the various forces acting on the hull, and v is the speed.

The rotation equation is based on the local coordinate system with the center of gravity as the origin, and the equation is as follows:

$$M \frac{\mathrm{d}\vec{\omega}}{\mathrm{d}t} + \vec{\omega} \times M\vec{\omega} = \vec{n} \tag{4}$$

$$M = \begin{bmatrix} M_{xx} M_{xy} M_{xz} \\ M_{xy} M_{yy} M_{yz} \\ M_{xz} M_{yz} M_{zz} \end{bmatrix} \tag{5}$$

where M is the moment of inertia of the transient state, $\vec{\omega}$ is the angular velocity of the hull, and $\vec{n}$ is the resultant moment acting on the hull.

In this study, the direct input method of boundary fluid velocity function is adopted for wave-making [19]. This boundary wave-making method is based on the velocity of wave water particle and the velocity of the inlet defined by the wave surface equation to achieve wave-making. This method can control wavelength, wave amplitude and wave frequency well, and the convergence of numerical simulation is good. For the target wave which is a planar linear sinusoidal regular wave in finite water depth, the relevant wave theoretical equation is expressed as follows, where the horizontal velocity equation is expressed as:

$$v_h = \zeta_a \omega \frac{chk(z + d_w)}{shkd_w} \cos k(x - ct) \quad (6)$$

The vertical velocity equation is:

$$v_v = \zeta_a \omega \frac{chk(z + d_w)}{shkd_w} \sin k(x - ct) \quad (7)$$

Where, ζ_a is wave amplitude; k is wave number; ω is circular frequency; d_w is water depth; c is velocity; t is time.

The wave period is defined as:

$$T = \frac{2\pi}{\omega} \quad (8)$$

The wavelength λ is defined as:

$$\lambda = \frac{2\pi}{K} \quad (9)$$

The relationship between wave period and wavelength under finite water depth is:

$$T = \left[\frac{g}{2\pi\lambda} \tanh\left(\frac{2\pi d}{\lambda}\right)\right]^{-1/2} \quad (10)$$

Where, λ is wavelength; g is gravitational acceleration; T is wave period.

For the processing of the flexible air seals at the bow and stern of the local air-cushion catamaran, this paper adopts the independent solver in STAR-CCM+, which is specially developed for the coupling effect of fluid and solid, namely fluid structure interaction (FSI), which makes it possible to calculate the linear or Nonlinear geometric deformation problems.

NUMERICAL CALCULATION MODEL

The traditional flexible device is used to seal the air at the bow and stern of the PACSCAT experimental model to achieve the purpose of lifting and reducing drag. The bow adopts bag-finger skirt, and the stern adopts double-bag skirt [1]. This configuration is able to not only ensure good airtightness of the air cushion, but also improve the obstacle-crossing performance and wave-breaking performance of PACSCAT. The sidewall is designed wide, the bow structure is similar to the gliding wall of a gliding boat [2] the cross structure is a pontoon structure used as a pressurized chamber. The schematic diagram of PACSCAT is shown in Fig. 1, and the principal dimension of the calculation model is shown in Table 1.

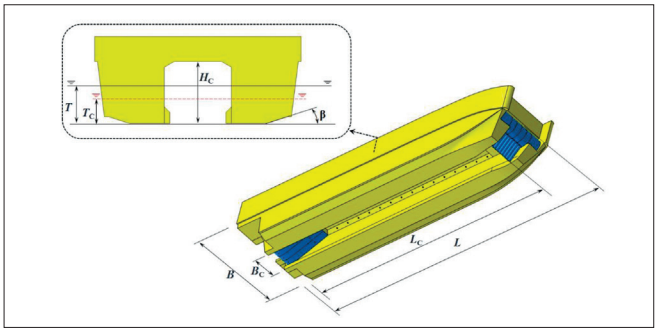

Fig. 1. Hull characteristics of PACSCAT

Tab. 1. The principal dimension of the calculation model.

Parameter	Model
Length L (m)	3
Breadth B(m)	0.7
Length of air cushion chamber Lc (m)	2.6
Breadth of sidewall B_1 (m)	0.22
Breadth of air cushion chamber B_C (m)	0.26
Height of cross structure Hc (m)	0.16

The air intake form of this study is pressurized chamber type, which is different from other hovercraft used air duct as high pressure air transmission method. The high pressure air enters into pressurized chamber directly after the fan pumping up, a part of air enters into air cushion chamber through a row of air hole in pressurized chamber, and the other part of high pressure air enters into air cushion chamber through the bow and stern air seals. The schematic diagram of air transportation of cushion system is shown in Fig. 2. When the air cushion system is numerically simulated, the air inlet is set at the top of the pressurized chamber, so that the high pressure air which is set as constant air flow will enter into pressurized chamber through the air hole connected with the air cushion chamber. The air intake form of numerical calculation is consistent with the experiment. To obtain the pressure situation of the air cushion chamber, pressure monitoring points P1, P2 and P3 are arranged at the fore, middle and rear positions of the air cushion chamber.

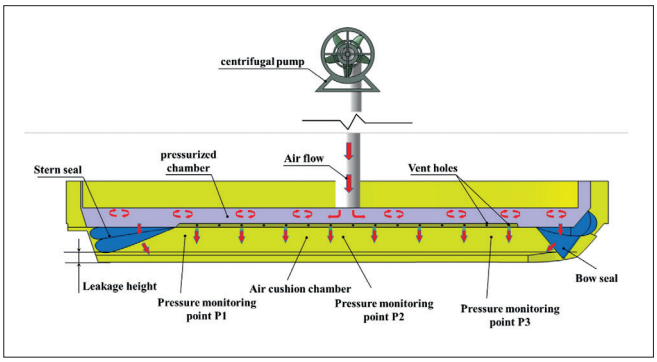

Fig. 2. Schematic diagram of cushion system in numerical calculation

CALCULATION DOMAIN AND GRID DIVISION

In order to represent correctly the experimental setup in the computational analyses, the hull in the computations was free to pitch and heave. In view of the hull characteristics of PACSCAT, the calculation domain adopts integral type to ensure the integrity of the air cushion system. For the simulation of flow field, the calculation domain is set to ensure the effective balance between calculation efficiency and accuracy as far as possible, and ensure that the wave-absorbing region is at least twice the wavelength. The selected wavelength in this study is 7 m. Therefore, the calculation domain is set as follows: The forward is 1 times the length of the ship, the aft is 3 times the

length of the ship, the side is 1 times the length of the ship, above the free liquid surface is 1 times the length of the ship, and below the free liquid surface is 1.5 times the length of the ship.

The inlet boundary condition of the calculation domain is Velocity inlet, and the outlet boundary condition is Pressure outlet. The top, bottom and both sides boundary condition of the calculation domain are set as slip wall, which named as Free slip wall. The calculated model is located near the free liquid surface as a 6-DOF rigid body. Fig. 3 shows calculation domain and boundary conditions. The VOF method is used to capture the movement of free liquid surface, and the wave pattern is first-order Stokes wave. The flow field in the calculation is Euler multiphase flow, continuum iteration is carried out by implicit unsteady state. The wave parameters in the calculation are exactly the same as those in the experiment, that is, the regular wave amplitude is 25 mm, and the ship speed is 2.0 m/s and 3.6 m/s, respectively.

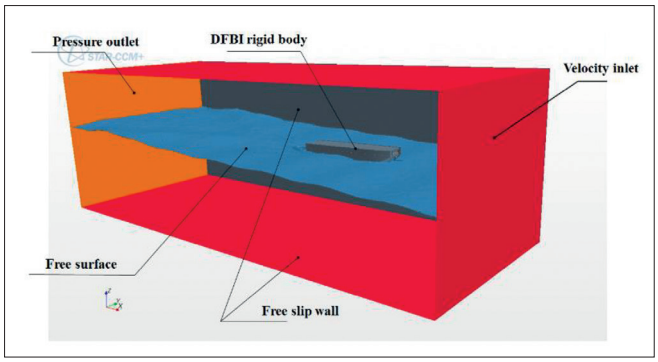

Fig. 3. Numerical calculation domain and boundary conditions

For the grid division, overlapping grid form is adopted in the study, and grid encryption is carried out at the area of free liquid surface, hull surrounding, cushion system and the bow and stern air seals. The wave height is set as 25 mm. The wavelengths of short wave and long wave to ship length ratio are quite different, so in order to capture the characteristics of wave better, the study adopts different division forms for grids at different wavelengths, so as to ensure that the number of grids per unit wavelength is not less than 70, and the number of grids per unit wave height is not less than 20 in the whole calculation domain [20]. Fig. 4 shows the division diagram of overlapping grids.

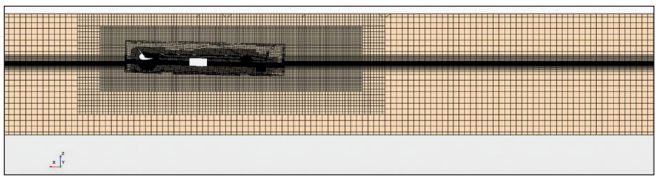

Fig. 4. The division diagram of overlapping grids

FLEXIBLE TREATMENT OF BOW AND STERN AIR SEAL

For flexible treatment of bow and stern air seals, fluid structure interaction method based on independent solver is used. However, mainly due to the high speed of the PACSCAT, flexible seals will cause the large deformation and the gas-liquid force changed, which makes the calculation impossible to be carried out, so the bow and stern gas seals needs some simplification. For the bow seals, rigid setting is carried out for the bow D type bag (shown as Fig. 5(a)), to simplify the force of the airbag and make numerical calculation more feasible, because in this study it cannot simulate the deformation of the flexible solid thin shell which has air and liquid on each side. The flexible finger skirts under real condition are composed of eight sets of independent skirt finger, as shown in Fig. 5(a). In the preliminary calculation, the author found that if the independent skirt fingers fit to each other nicely, the grid treatment will encounter mutual interference problems, especially at the junction, the limited fluid force cannot be obtained because of the extremely small gap, and the calculation cannot be performed. Based on the preliminary calculation results, the flexible finger skirts are processed that each independent finger does not stick, and each shirt has a gap of about 2.5 mm wide, with 2.28 mm thickness, as shown in Fig. 5(b). Usually, the skirts near the sidewall of PACSCAT will not deform in the real condition, besides that, the deformable treatment will lead to the non-convergence of numerical calculation, so the wall surface of finger skirt at the junction of sidewall is set as a rigid structure, which is made non-adhesion treatment with the rigid sidewall.

For the stern air seal structure, considering that it is currently impossible to couple the double airbags in the inflated state in the case of triple media such as gas, liquid, and solid, as shown in Fig. 6(a), so it is necessary to simplify the stern airbag by a flat

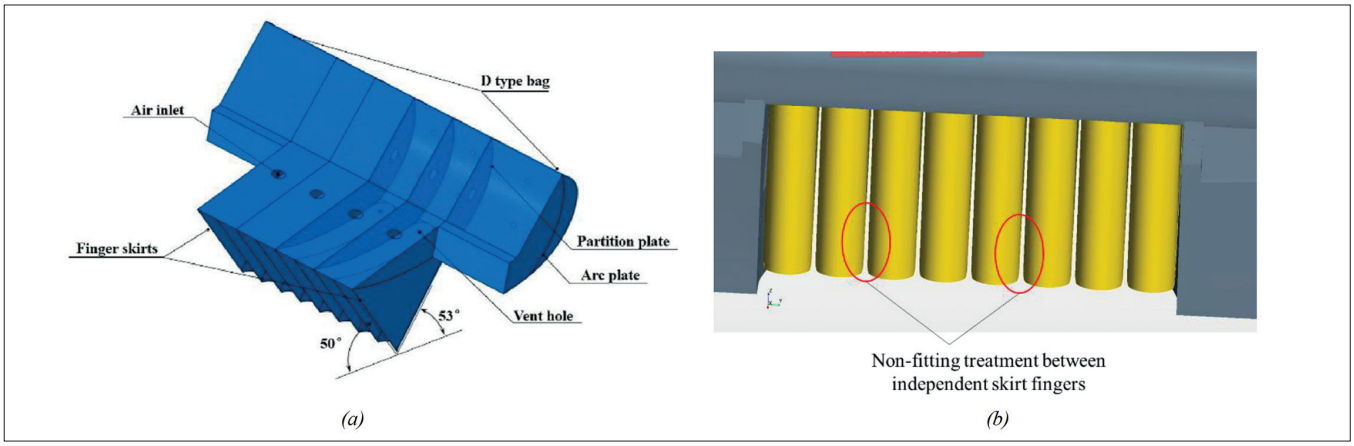

Fig. 5. Non-adherent treatment of bow skirt finger

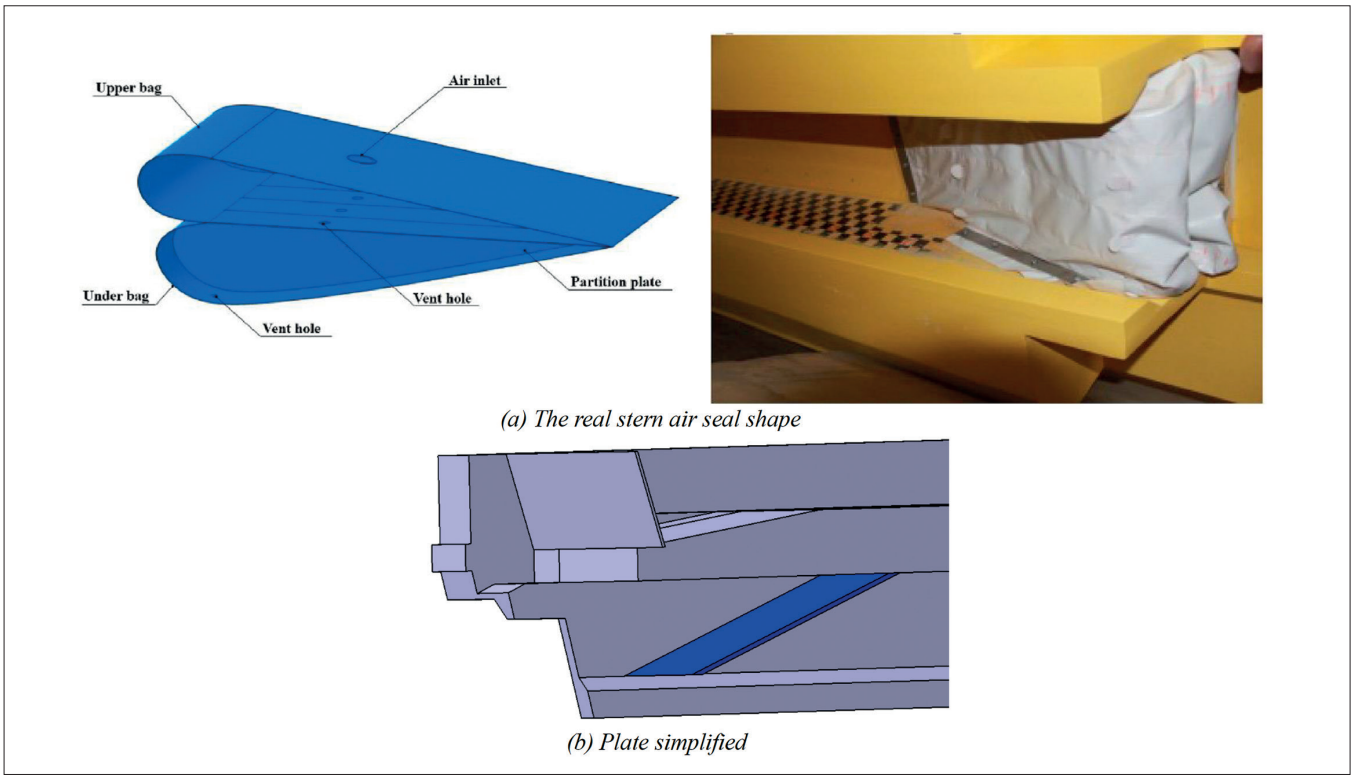

Fig. 6. The real and simplified of stern double bag air seal

plate in this study. In order to match the flexible characteristics of the double-bag stern seals, and according to the expression of the stiffness of the elastic material in the force analysis of the flexible air seal, this study carried out preliminary calculations to determine the optimal material characteristic parameters by comparing the resistance error in waves. The calculations were based on the same Poisson coefficient and model scale, for flexible plates with different Young's modulus and different densities. And then the properties of the bow and stern gas seal material used are selected as a density of 1300 kg/m3, a Young's modulus of 10 MPa, and a Poisson coefficient of 0.45. During the calculation, it is found that the stern flexible plate with uniform density and thickness is more conducive to the realization of numerical calculation, so the stern flexible plate air seal set here is uniform, and the thickness of the plate is 7mm, as shown in Fig. 6(b). It should be noted that the flat-type simplification of the double-bag stern seals can only achieve the purpose of sealing the air-cushion cabin, and cannot fully simulate the double-bag seals in the real situation.

In contrast to the single flow field calculation domain for rigid air seals, fluid structure interaction calculation domain requires to define multiple domains for interactions and fluid motions between different fluids and solids. Due to the large increase of the number of flexible air seal grids, the balance of calculation and analysis between the grid number and calculated efficiency must be considered. The follow-up work of this paper is to study the number of grids which are used in the final calculation. Figs. 7 and 8 below show the grid form of the bow and stern air seal.

Because the hull of PACSCAT is a 6-DOF rigid body that is non-deformable solid, so the ship does not need a solid area, only the deformable bow and stern air seal need solid areas. These areas are connected by the following interfaces: A fluid-structure interface between the bow air seal and the fluid

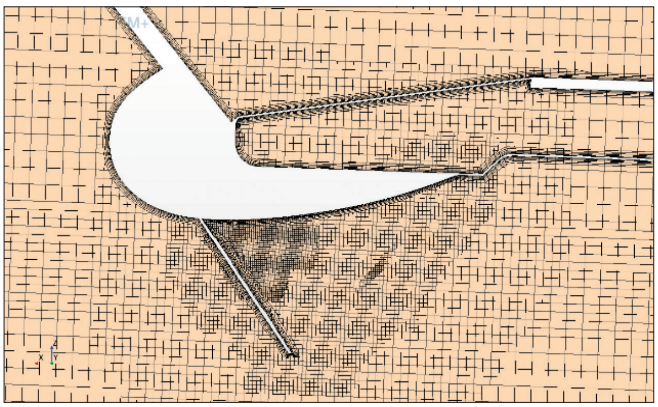

Fig. 7. The grid form of bow skirt

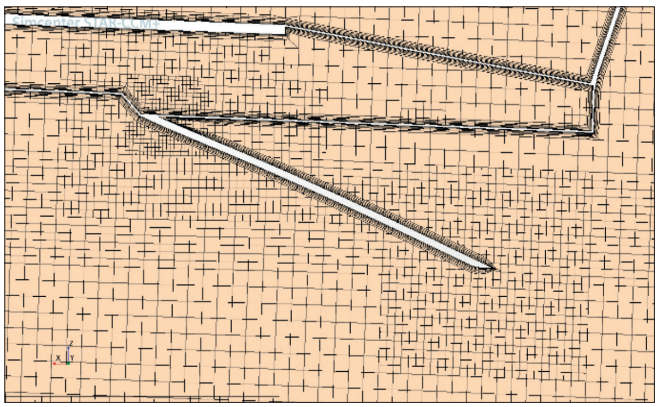

Fig. 8. The grid form of stern skirt

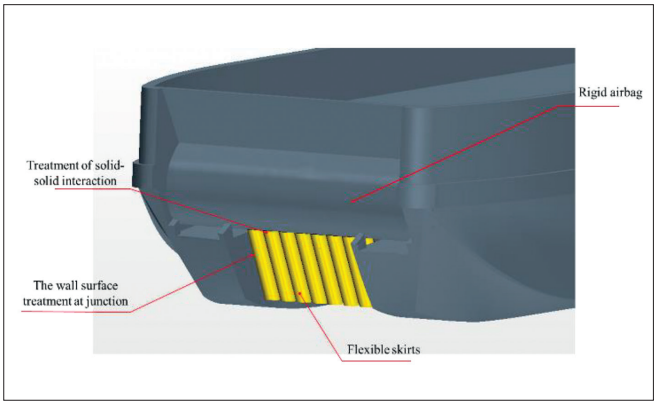

Fig. 9. Interface of bow air seal

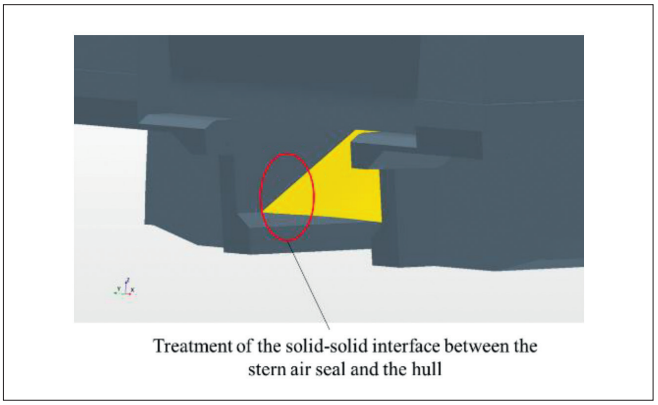

Fig. 10. Interface of stern air seal

surrounding the air seal; A fluid-structure interface between the stern air seal and the fluid surrounding the air seal; A fluid-fluid interface between the fluid area of main body and the fluid surrounding the bow and stern air seals; A solid-solid interface between different solid parts of bow and stern air seals. As shown in Figs. 9 and 10 below, the solid-solid interface treatment between the top of skirt finger and the rigid airbag of the bow skirt will be carried out; and the solid-solid interface treatment between the top of stern simplified plate and the wet deck of the air cushion chamber will be carried out.

CALCULATION RESULTS AND ANALYSIS

COMPARISON BETWEEN NUMERICAL CALCULATION AND EXPERIMENTAL DATA

Figures 11 to 12 are the time histories of the calculated values of heave and pitch compared with the experimental values in waves, when the speed is 3.6 m/s and the wavelength is 7.0 m. In order to analyze the calculation results, the calculation time histories are linearized by using the sine curve fitting method. It can be seen from Fig. 11 that the calculated value and the experimental value are relatively close in terms of amplitude and mean, and the curves have similar motion characteristics. From the Fig. 12, it can be seen that the calculated data and phase are basically consistent with the experimental results, and the calculated mean value is relatively close to the experimental value. Comparing the heave and pitch curves, the following conclusions can be drawn: In the numerical calculation of the PACSCAT with flexible seals based on the fluid structure interaction (FSI), the motion characteristics of each motion parameter are close to the experimental values. Although there is a certain error in the amplitude, the motion of heave and pitch law have obvious similarity, and the mean error is small, indicating that the method is feasible to the study of flow field characteristic analysis of PACSCAT.

The air cushion pressure is an important parameter of the cushion system directly affects its performance, especially when the pressure jump is large due to the unsteady leakage. In this study, the accuracy of air cushion pressure numerical simulation is studied by comparing with the experimental data, meanwhile the pressurized chamber pressure and air cushion pressure at low speed are calculated extended, so that the pressure characteristics of PACSCAT in waves can be analysed.

Fig. 13 shows the comparison between the calculated values and the test values of air cushion pressure at the wavelength of 7.0 m and speed of 3.6 m/s. The pressure of pc1, pc2 and pc3 is the pressure value of P1, P2 and P3 mentioned above, EXP is the test data, and CAL is the numerical calculated data. As shown as the Fig. 13, the nonlinear characteristics of numerical calculation are not as obvious as the test values, and the oscillation amplitudes of the time histories of numerical calculation are quite slight, such as the calculation value at pc1, which is always around 0.8kpa. The oscillation pattens of the calculated data are close to each other at different longitudinal positions of the air cushion, especially the peak value and trough value of pc2 are more obvious. The nonlinear oscillation characteristics of the test values are more prominent, the main reason is that the non-uniform leakage phenomenon caused by the flexible air seal of the bow and stern is more obvious, and the dynamic response of the simulated bow and stern flexible air seals is quite different from that of the actual air seals, so the

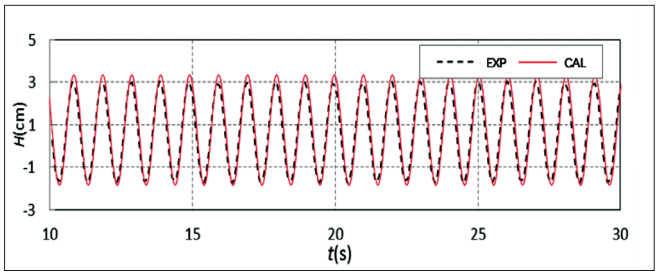

Fig. 11. Comparison of wave time histories curves between calculated heave values and test values

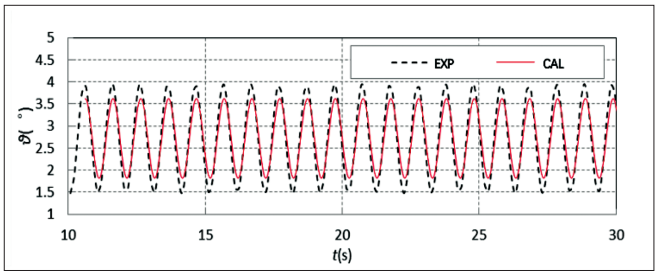

Fig. 12. Comparison of wave time histories curves between pitch values and test values

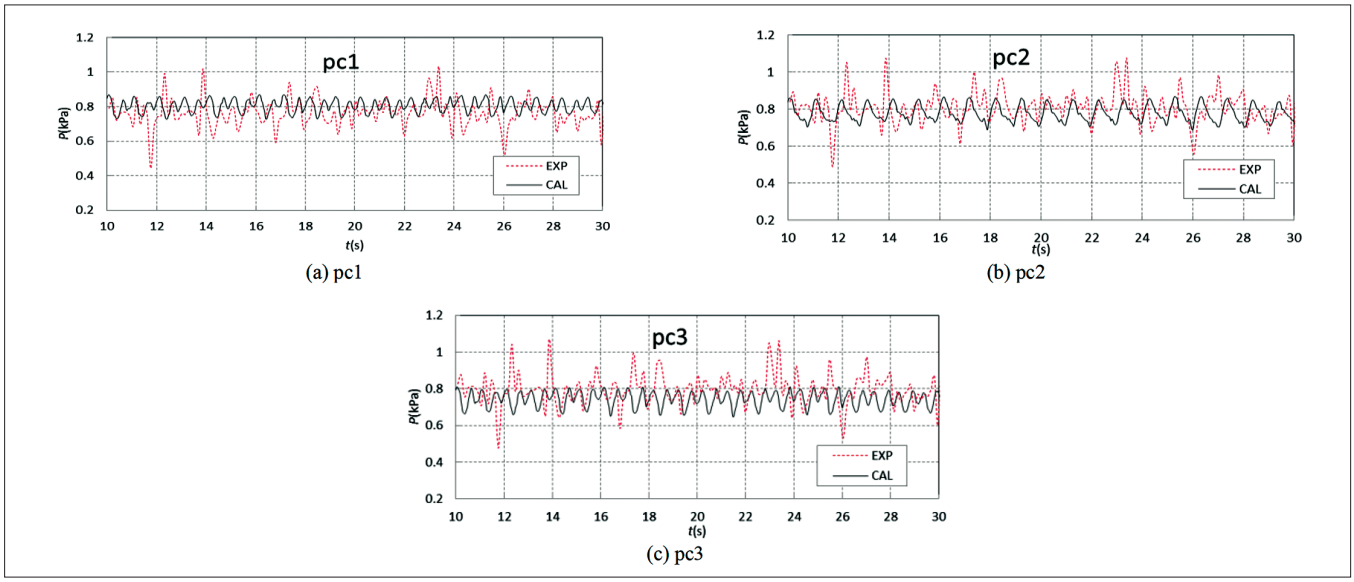

Fig. 13. Comparison of original test and calculated values of air cushion pressure at different positions of air cushion

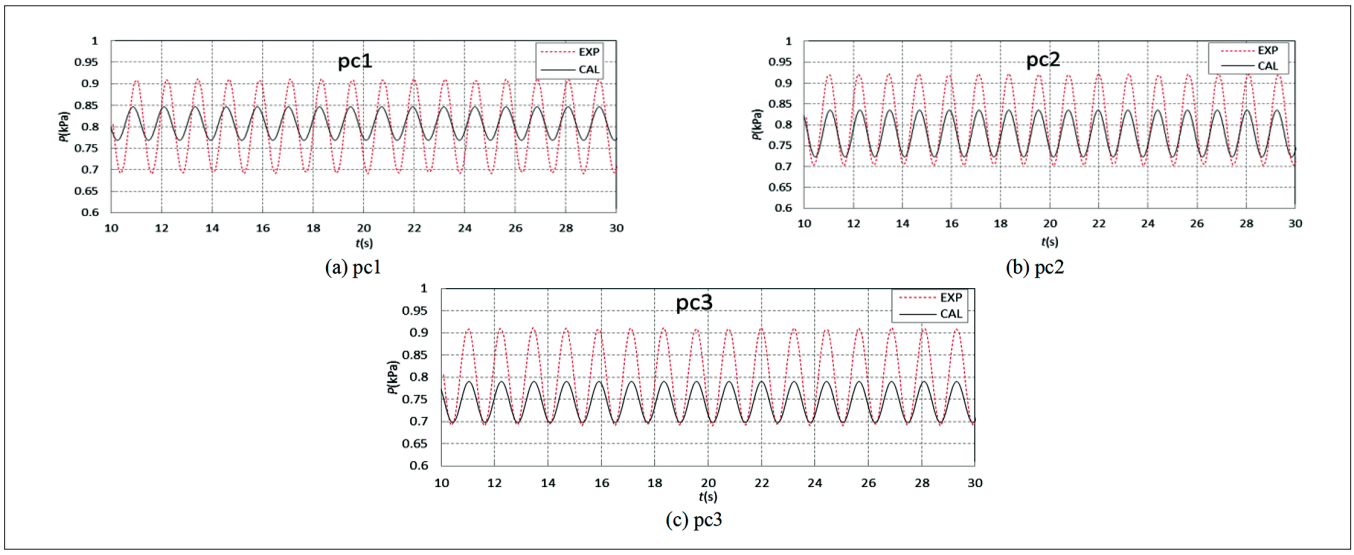

Fig. 14. Comparison of linearized test and calculated values of air cushion pressure at different positions of air cushion

flexible state of the bow and stern air seals cannot be completely simulated, which makes the oscillation relatively gentle. Fig. 14 shows the comparison of data after linear transformation. It can be seen that the oscillation amplitudes of the test values are significantly larger than the calculated values. The amplitudes of the test values at different positions are close to each other, and that of the calculated values are also close to each other. Compared with the amplitudes, the calculated average values are closer to the test values, especially at the longitudinal position p1 of the air cushion. With the moving forward of the air cushion pressure point, the calculated average values decrease gradually, and the errors between the calculated values and the test values increase gradually. The pressure data of the numerical calculation at the fore of the air cushion is lower than that at the aft. The main reason is that the air seal treatment at the bow based on fluid structure interaction adopts the form of independent skirt fingers, and there is a certain gap between each skirt finger, which leads to a certain amount of air cushion leakage, then affects the changes of pressure.

COMPARISON OF PRESSURE CALCULATION RESULTS AT DIFFERENT SPEEDS

According to the above introduction, the sailing attitude of PACSCAT at low speed is quite different from that at high speed, and the air cushion pressure is also quite different. In this section, the model at a wavelength of 7.0 m and a speed of 2.0 m/s is studied, the air cushion pressure is compared to that of speed at 3.6 m/s, and the characteristics of air cushion pressure at low speed and high speed are analysed. Fig. 15 shows the comparison of the original calculation data at different speeds and different pressure points, it can be seen that both average and amplitude of air cushion pressure at the speed of 2.0 m/s are significantly reduced than that at the speed of 3.6 m/s, the variation curves of pressure at low speeds and different positions are relatively consistent, and the air cushion pressure is evenly distributed in the air cushion space at low speed. It indicates that there is no obvious air leakage when the ship sails in the wave in this momen.

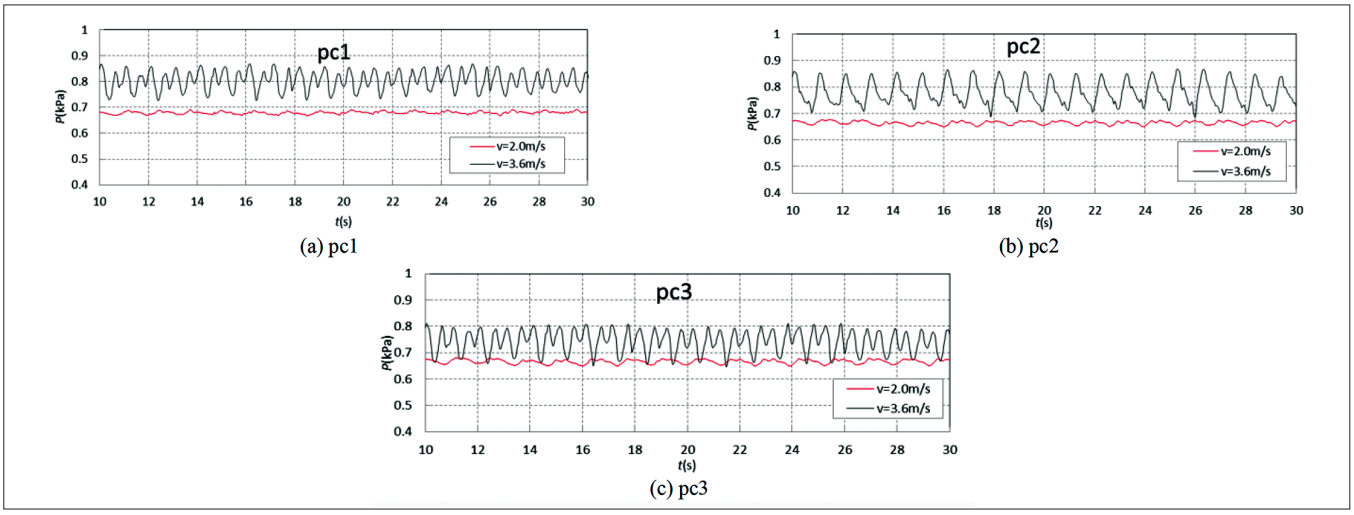

Fig. 15. Comparison of original calculated data of air cushion pressure at different speeds

PRESSURE CHARACTERISTIC ANALYSIS OF PRESSURIZED CHAMBER

As for the cushion system, the pressurized chamber mainly plays the role of combining and conveying high pressure air to the air cushion chamber. In general, different with the force exerted on the air cushion chamber when contacting with waves, the pressure fluctuation in the pressurized chamber is caused only by the reaction force of the air cushion pressure. This section studies the pressure fluctuation of the pressurized chamber in waves and analyses its diachronic characteristics at different speeds. The calculated pressure points are distributed at the three spatial points arranged at the fore, middle and rear of the pressurized chamber. The longitudinal coordinate positions are consistent with P1, P2 and P3 of the air cushion chamber, and the vertical positions are in the middle positions between the upper and lower decks of the pressurized chamber. The pressure is marked as Pt1, Pt2 and Pt3 respectively. There is no linearization treatment to the calculated data in order to analyse the pressure of the pressurized chamber from the perspective of the original calculated data. Figs. 16 and 17 respectively show the pressure monitoring condition in the pressurized chamber at the speed of 2.0 m/s and 3.6 m/s at different positions, and the air cushion pressure pc2 in the Figure is displayed for comparative analysis. It can be seen from Fig. 16 that the pressure duration of the three monitoring points in the pressurized chamber are almost the same in terms of amplitudes, average values, and oscillation pattens, indicating that the pressurized chamber pressure is little disturbed by the change of air cushion pressure at low speed, and the amplitude of pressurized chamber pressure and air cushion pressure pc2 is basically the same. At this time, the average ratio of pressurized chamber pressure to air cushion pressure is 1.034. In Fig. 17, the time histories of pressurized chamber pressure at the three monitoring points are complex and do not show the same variation laws, but the amplitude is close to the average value, and there is no significant difference between the amplitude at pc2. At this time, the average ratio of pressurized chamber pressure to air cushion pressure is 1.303. Contrast with the condition at different speeds, the pressure curve characteristics of pressurized chamber have similarities with the air cushion pressure in previous section, but pressurized chamber pressure is closer to air cushion pressure at lower speed, and much greater than air cushion pressure obviously at higher speed, so that the ratio of pressurized chamber pressure to air cushion pressure up to 1.3. It follows that when PACSCAT sailing in waves, high speed will cause pressure changes in the pressurized chamber or the air flue, researchers need to pay more attention to the design of the pressurized chamber, so as to avoid the phenomenon of fan pumping due to excessive pressure.

No matter at low speed and high speed, the pressurized chamber pressure at three monitoring points is similar, so the pressurized chamber pressure in space is evenly distributed well, which has the effect of combining the high pressure air to a certain extent, thereby avoiding delivery timeliness reducing due to spatial non-uniform distribution of the air, and then affecting the lift performance.

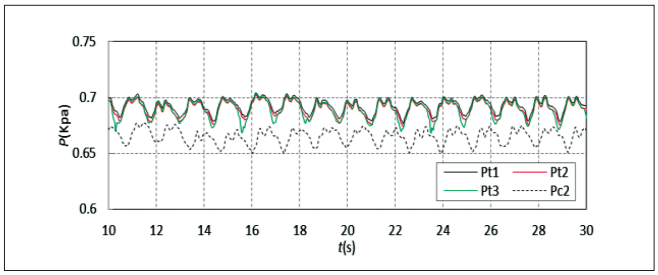

Fig. 16 Calculation data of pressure in pressurized chamber at different positions at speed V =2.0 m/s

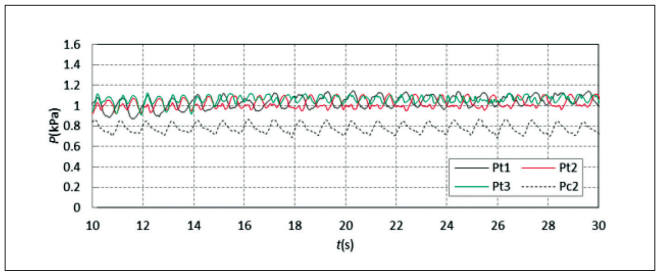

Fig. 17. Calculation data of pressure in pressurized chamber at different positions at speed V =3.6 m/s

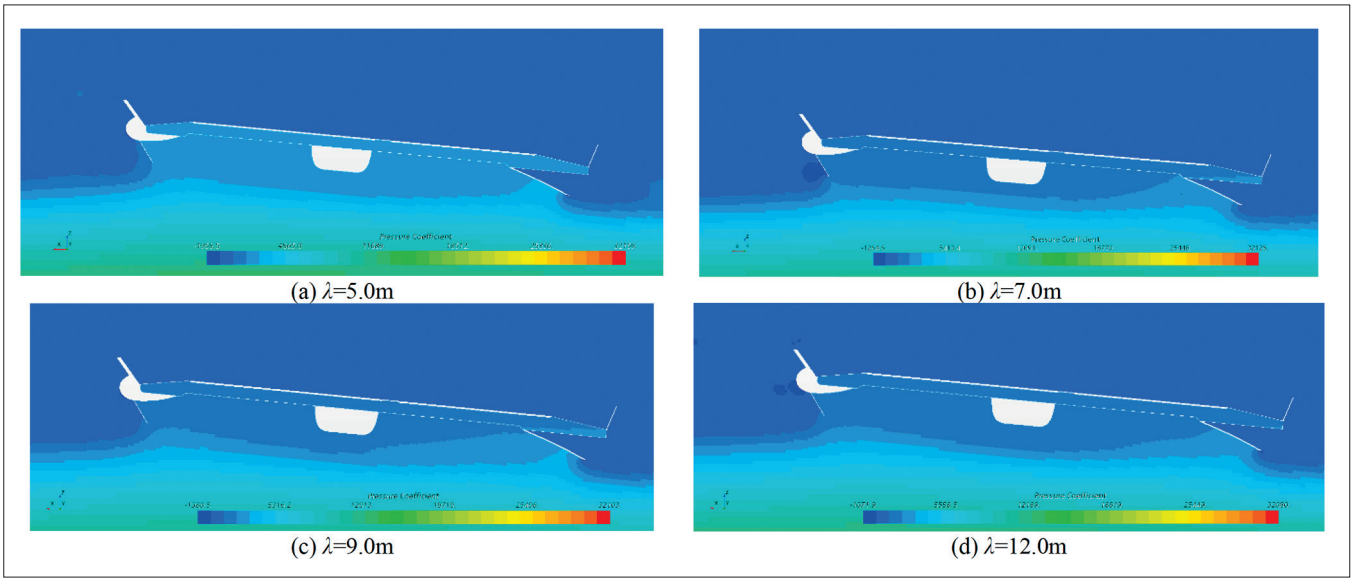

Fig. 18. Vertical spatial pressure distribution at speed V =3.6m/s

SPATIAL PRESSURE DISTRIBUTION CHARACTERISTICS

The pressurized chamber and air cushion chamber pressure at different positions are analysed by monitoring points in the previous section, the spatial pressure in air cushion chamber will change with the waves and the attitude of hull, the air cushion of the system usually assume evenly distributed in space, this section will analyse the pressure nephogram of the system, and study the uniform distribution of air cushion in space at different speeds. Fig. 18 below shows the pressure nephogram of air cushion in vertical space at different wavelengths and at the speed of 3.6 m/s, the transverse position of nephogram is just at Y = 0. The air cushion pressure in the vertical direction has little change in the pressurized chamber and air cushion chamber, especially the pressure in the pressurized chamber. There is a certain pressure fluctuation at the rear of the air cushion chamber, the fluctuation range is concentrated at the middle and rear of the longitudinal positions, the pressure fluctuation does not reach the wet deck of the air cushion chamber, so it can be considered that the pressure at the rear of the air cushion chamber is almost evenly distributed in space except at the stern air seal position.

Fig. 19 and 20 below respectively show the spatial pressure distribution in xy plane of pressurized chamber and air cushion chamber, it can be seen from the Fig. 17, the air cushion pressure of pressurized chamber in the xy plane is almost the same, according to the monitoring situation of pressure duration curve at different positions in the previous section, the air cushion pressure in the pressurized chamber is evenly distributed for sure, and the disturbance caused by wave force is small. It can be seen from Fig. 18 that the air cushion pressure has a sudden jump at the fore and rear positions, especially near the stern air seal. From the vertical spatial pressure distribution of the air

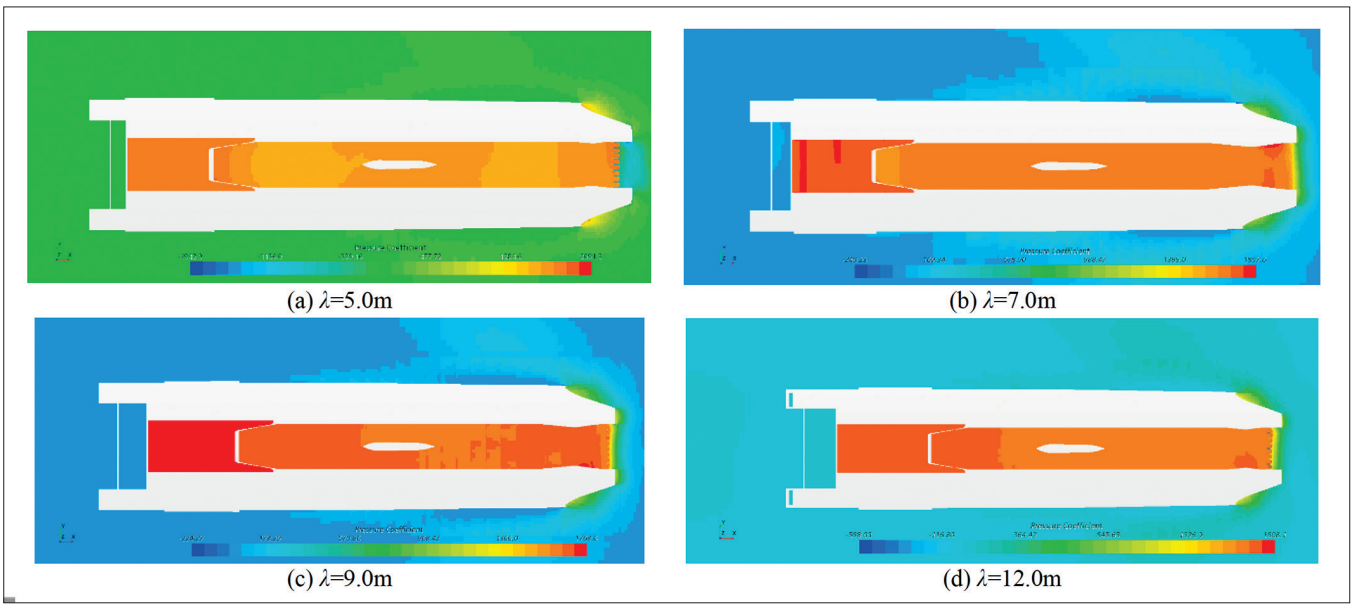

Fig. 19. Pressure distribution of pressurized chamber in the xy plane at the speed of V =3.6m/s

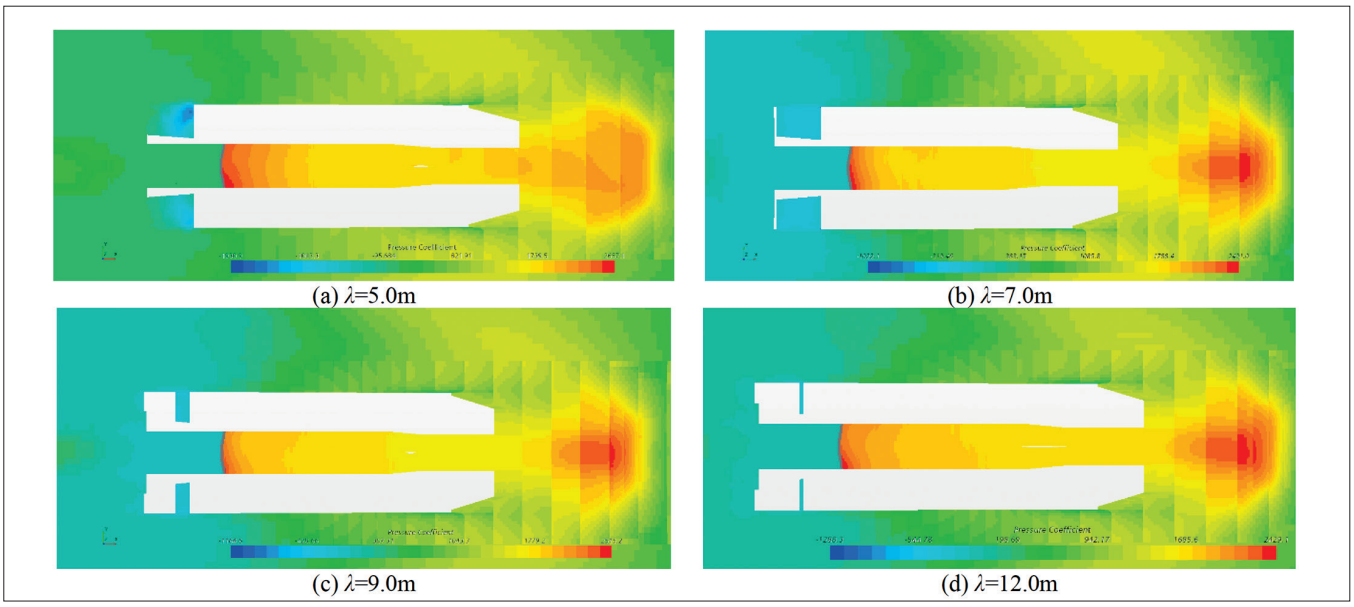

Fig. 20. Pressure distribution of air cushion chamber in the xy plane at the speed of V =3.6m/s

cushion chamber in Fig. 16, it is not difficult to understand that the pressure is obviously larger here. Therefore, the conclusion can be basically consistent with the above, that is, except for the position near the stern air seal, the pressure in most space of the air cushion chamber is evenly distributed.

Figs. 21 and 23 show the spatial pressure distribution at wavelength of 5.0 m and 7.0 m at the speed of v=2.0 m/s, so as to study the characteristics of the spatial pressure characteristics in the air cushion chamber at low speed. From the comparative analysis of the vertical and xy plane pressure nephogram, it can

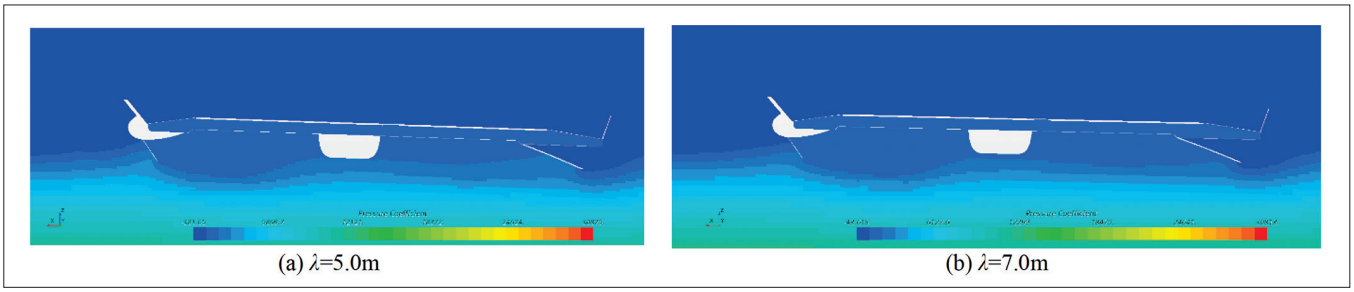

Fig. 21. Vertical spatial pressure distribution at speed of V =2.0m/s

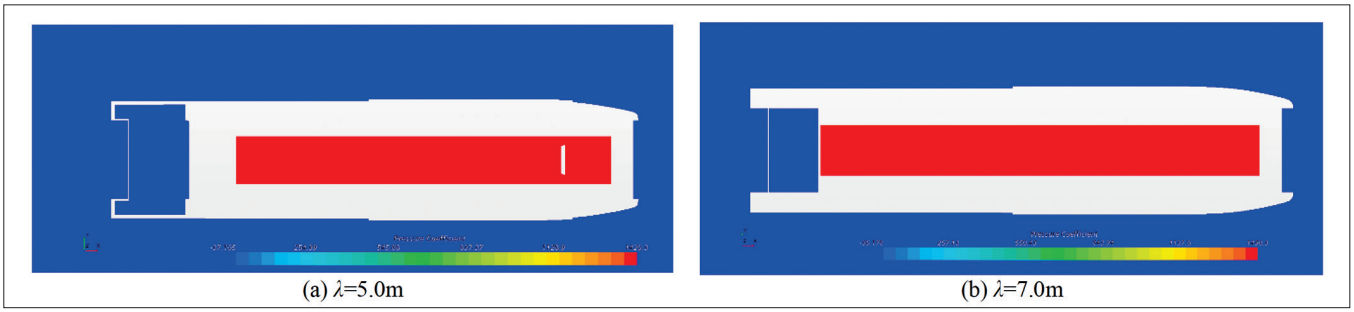

Fig. 22. Pressure distribution of pressurized chamber in the xy plane at speed of V =2.0m/s

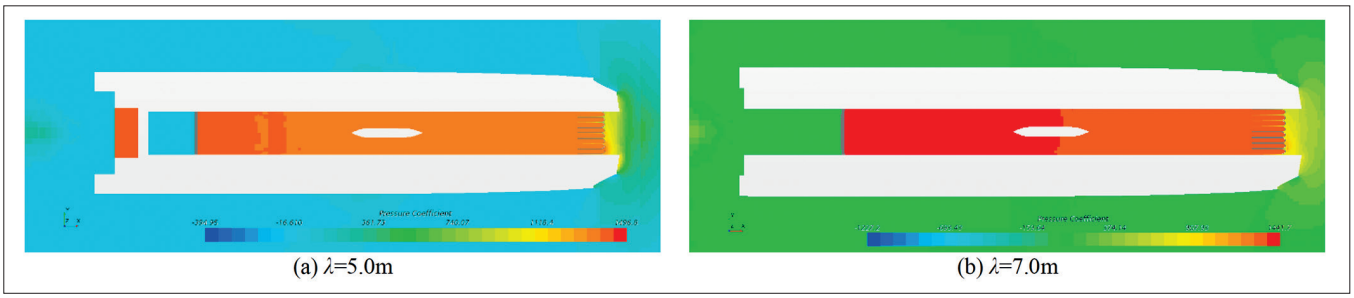

Fig. 23. Pressure distribution of air cushion chamber in the xy plane at speed of V =2.0m/s

be clearly seen that at this speed, the pressure no matter in the pressurized chamber or in the air cushion chamber is uniformly distributed in space, especially in the pressurized chamber, the pressure changes are slight. Therefore compared with the uniform distribution condition of air cushion space at speed of 3.6 m/s, a conclusion can be carried out as follows, when PACSCAT sailing in waves at low speed, the spatial pressure distribution is evenly distributed no matter in the pressurized chamber or in the air cushion chamber, and the wave disturbance is slight, but at high speed, the pressure in the pressurized chamber is evenly distributed, the pressure in air cushion chamber is also considered to be uniform distribution except near the stern air seal position where occurs a pressure jump. The spatial uniform distribution of pressure also indicates that the arrangement with gap between each skirt finger does not cause excessive leakage of air and a large change of air cushion pressure.

CONCLUSIONS

This study calculates the variation performance of the cushion system pressure, in waves at different wavelengths and speeds, based on the flow field characteristics of PACSCAT cushion system by using the fluid structure interaction method, and the conclusions are as follows:

a) The nonlinear characteristics of the numerical calculation of the pressure in the air-cushion cabin are relatively low, the oscillation amplitudes of the time histories of numerical calculation are smaller. The oscillation pattens of the original calculated data at different longitudinal positions of the air cushion are similar, especially the peak value and trough value at pc2 are more prominent.
b) After linear processing, the oscillation amplitudes of air cushion chamber pressure test values are larger than the calculated values, in comparison with the amplitudes, the average of calculated values are more close to the experimental values, especially at the longitudinal position P1 of air cushion, and with the air cushion pressure point moving forward, the average calculated values reduce gradually, and the calculation deviation also gradually increases.
c) When PACSCAT sailing at low speed, the spatial pressure is uniformly distributed and less disturbed by waves no matter in the pressurized chamber or the air cushion chamber, while PACSCAT sailing at high speed, except for the pressure jump in the air cushion chamber near the stern air seal position, the pressure in other spaces is also considered to be uniformly distributed.

REFERENCES

1. L. Yun, and A. Bliault, *Theory and design of air cushion craft.* London: Bath Press, 2000.

2. J. Zou, Q.J. Meng, Z. Lin, and X.W. Li, "Research on the concept of PACSCAT," *Ship Science and Technology*, vol. 34, no. 7, pp. 30-34, July 2012, doi: 10.3404/j.issn.1672-7649.2012.07.006

3. B. Milewski, B. Connell, J. Wilson, and D. Kring, "Dynamics of ACV operating in a seaway," in *Proc. of the 9th Int. Con. on Numerical Ship Hydrodynamics, 5-8 August 2007, Ann Arbor*, USA [Online]. Available: https://citeseerx.ist.psu.edu/viewdoc/summary?doi=10.1.1.547.1611

4. W.M. Milewski, B. Connell, B. Petersen, and D. Kring, "Initial validation of the ACVSIM model for dynamics of air cushion vehicles," in *Proc. of the 27th Symposium on Naval Hydrodynamics, 5-10 October 2008, Seoul, Korea*, 2008. [Online]. Available: https://citeseerx.ist.psu.edu/viewdoc/summary?doi=10.1.1.511.2009

5. WAMIT Inc. *WAMIT User Manual-Version 7*. Chestnut Hill, 2016.

6. C.H. Lee, and J.N. Newman, "An extended boundary integral equation for structures with oscillatory free-surface pressure," *International Journal of Offshore and Polar Engineering*, vol. 26, no. 1, pp. 41-47, 26(1): 41-47, March 2016, doi: 10.17736/ijope.2016.mk44

7. N. Hirata, and O.M. Faltinsen, "Computation of cobblestone effect with unsteady viscous flow under a stern seal of a SES," *Journal of Fluids and Structures*, vol. 14, no. 7, pp.1053-1069, October 2000, doi: 10.1006/jfls.2000.0312

8. G.L. Li, "Analysis of heave characteristics of SES in short wave," *Jiangsu Ship*, vol. 13, no. 3, pp. 1-7, June 1996, doi: CNKI:SUN:JSCB.0.1996-03-000

9. Z.Q. You, *Numerical simulation and optimization of internal Flow field of ACV*. Harbin Engineering University, 2018.

10. K.J. Chen, *Research on CFD calculation method of cushion lift performance of hovercraft*. Dalian University of Technology, 2013.

11. B. Lan, *CFD calculation of hydrodynamic performance of cushion lift platform*. Harbin Engineering University, 2006.

12. W.Y. Duan, and S. Ma, "Comparison of two -, two - and half - and three - dimensional methods for hydrodynamic linear solutions of ship motion," in *Proc. of the 17th National Symposium on Hydrodynamics, 31 December 2003 – 2 January 2004, HongKong, China*. [Online] Available: https://d.wanfangdata.com.cn/

13. Z.Q. Guo, *Multi-domain 2.5D method with viscous effects and its application on a partial air cushion supported catamaran*. Harbin Engineering University, 2017.

14. W.Y. Wu, *Hydrodynamic*. Beijing: Peking University Press, 1982.

15. F.J. Wang, *Calculated hydrodynamic analysis*. Beijing: Tsinghua University Press, 2004.

16. C.S. Wu, and D.X. Zhu, "Numerical simulation of sailing ship radiation problem based on N-S equation," *Journal of Ship Mechanics*, vol. 12, no. 4, pp. 560-567, September 2008, doi: JournalArticle/5aed43dcc095d710d40a20e8

17. L. Lei, Z.X. Wang, P. Sun, and J.N. Nie, "Application research of ideal equation turbulence model for computational fluids," *Ship Engineering*, vol. 2010, no. 3, pp. 5-8, June 2010.

18. Y.B. Li, D.B. Huang, and Y. Liang, "A theoretical calculation method for far field waveform of hovercraft," *Journal of Harbin Engineering University*, vol. 23, no. 2, pp. 5-7, February 2002, doi: 10.3969/j.issn.1000-6982.2010.03.002

19. J.D Li, *Seakeeping*. Harbin: Harbin Institute of Ship Engineering Press, 1992.

20. R. Deng, *Numerical research on influence of the interceptor on catamaran hydrodynamic performances*. Harbin Engineering University, 2010.

CONTACT WITH THE AUTHORS

Jinglei Yang
e-mail: yangjinglei1220@126.com
Jimei University
School of Marine Engineering, Xiamen
China

Han-bing Sun

Jimei University
School of Marine Engineering, Xiamen
China

Xiao-wen Li

Jimei University
School of Marine Engineering, Xiamen
China

Xin Liu

Jimei University
School of Marine Engineering, Xiamen
China